



OPEN ACCESS

EDITED BY

Maolin Lu,
University of Texas at Tyler Health Science
Center, United States

REVIEWED BY

Zaid A. Abassi,
Technion Israel Institute of Technology, Israel
Yasuteru Sakurai,
Nagasaki University, Japan

*CORRESPONDENCE

Barbara Schmidt
✉ barbara.schmidt@ukr.de

RECEIVED 31 October 2025

REVISED 17 December 2025

ACCEPTED 22 December 2025

PUBLISHED 12 January 2026

CITATION

Magnus CL, Jaber ZH, Hiergeist A, Arnold L, Marchel H, Lamprecht A, Hanses F, Dienemann T, Schneckenpointner R, Lubnow M, Müller T, Lunz D, Hitzenbichler F, Schmid S, Müller M, Poeck H, Graf B, Salzberger B, Gessner A, Schmidt B and Schuster P (2026) SARS-CoV-2 evolution enhances endocytic uptake while preserving TMPRSS2-dependent fusion. *Front. Immunol.* 16:1736891. doi: 10.3389/fimmu.2025.1736891

COPYRIGHT

© 2026 Magnus, Jaber, Hiergeist, Arnold, Marchel, Lamprecht, Hanses, Dienemann, Schneckenpointner, Lubnow, Müller, Lunz, Hitzenbichler, Schmid, Müller, Poeck, Graf, Salzberger, Gessner, Schmidt and Schuster. This is an open-access article distributed under the terms of the [Creative Commons Attribution License \(CC BY\)](https://creativecommons.org/licenses/by/4.0/). The use, distribution or reproduction in other forums is permitted, provided the original author(s) and the copyright owner(s) are credited and that the original publication in this journal is cited, in accordance with accepted academic practice. No use, distribution or reproduction is permitted which does not comply with these terms.

SARS-CoV-2 evolution enhances endocytic uptake while preserving TMPRSS2-dependent fusion

Clara L. Magnus¹, Zeliha Hamed Jaber¹, Andreas Hiergeist², Lisa Arnold¹, Harriet Marchel², Antonia Lamprecht², Frank Hanses^{3,4}, Thomas Dienemann⁵, Roland Schneckenpointner⁶, Matthias Lubnow⁶, Thomas Müller⁶, Dirk Lunz⁷, Florian Hitzenbichler⁴, Stephan Schmid⁸, Martina Müller⁸, Hendrik Poeck^{9,10}, Bernhard Graf⁷, Bernd Salzberger⁴, André Gessner^{1,2}, Barbara Schmidt^{1,2*} and Philipp Schuster²

¹Institute of Clinical Microbiology and Hygiene, University Hospital Regensburg, Regensburg, Germany,

²Institute of Medical Microbiology and Hygiene, University of Regensburg, Regensburg, Germany,

³Emergency Department, University Hospital Regensburg, Regensburg, Germany, ⁴Department of

Infection Prevention and Infectious Diseases, University Hospital Regensburg, Regensburg, Germany,

⁵Department of Surgery, University Hospital Regensburg, Regensburg, Germany, ⁶Department of Internal

Medicine II, University Hospital Regensburg, Regensburg, Germany, ⁷Department of Anesthesiology,

University Hospital Regensburg, Regensburg, Germany, ⁸Department of Internal Medicine I, University

Hospital Regensburg, Regensburg, Germany, ⁹Department of Department of Internal Medicine 3,

University Medical Center, Regensburg, Germany, ¹⁰Leibniz Institute for Immunotherapy,

Regensburg, Germany

Background: Of the five SARS-CoV-2 variants-of-concern (VOC), Omicron shows increased transmissibility and infectivity, but lower pathogenicity. This drop in virulence was associated with an altered entry of VOC Omicron into airway epithelia by endocytosis instead of direct fusion, increasing virus replication in the upper airways and decreasing spread to the lower respiratory tract.

Methods: We aimed to assess the extent of direct fusion and endocytosis in nine clinical SARS-CoV-2 isolates collected during the SARS-CoV-2 pandemic, comprising wild-type (n=1), Alpha (n=2), Delta (n=1), and Omicron (n=5) strains. Viral entry was investigated in four different human cell lines in the presence of camostat, an inhibitor of TMPRSS2-mediated fusion, and aloxistatin, a cathepsin protease inhibitor blocking viral endocytic entry (0.024-100 μ M). Full-length viral genomes were obtained using next generation sequencing.

Results: Alpha and Delta variants predominantly entered Calu-3 and Caco-2 cells through TMPRSS2-dependent membrane fusion, whereas Omicron variants – particularly BE.1.1 and BA.5 – showed a pronounced shift toward endocytosis in A549^{hACE2+/TMPRSS2+} and HEK293T cells. Endocytic uptake was preferentially utilized by strains carrying Δ 69/ Δ 70 and L452R in combination with F486V.

Conclusions: All Omicron variants retained TMPRSS2-dependent fusion activity, indicating that VOC Omicron broadened rather than shifted its cell tropism. While replication in the upper airways and transmissibility are enhanced, the

capacity to infect the lower respiratory tract is preserved, which may pose a risk for immunocompromised individuals. The combination of $\Delta 69/\Delta 70$, L452R, and mutations at position 486 may confer a selective advantage, as this constellation is now prevalent in nearly all circulating SARS-CoV-2 lineages.

KEYWORDS

coronavirus, endocytosis, evolution, fusion, SARS-CoV-2, tropism, variants-of-concern, viral entry

1 Introduction

Since its first appearance in Wuhan, China, at the end of 2019 (1, 2), SARS-CoV-2 has spread worldwide and has since gradually adapted to the human host and its humoral and cellular immune responses (3). The original strain and in particular subsequent variants-of-concern (VOC) Alpha (B.1.1.7) and Delta (AY.33) were associated with a high morbidity and mortality (4, 5). In contrast, VOC Omicron, which occurred concurrently with mass vaccination, showed much higher infectivity with lower disease severity, at least in patients without comorbidities and without immunosuppression (6, 7).

The entry of SARS-CoV-2 into target cells requires cleavage of the spike protein into S1 and S2 subunits by furin or furin-like proteases in the virus-producing cell. The nascent virus binds to ACE-2 with its S1 receptor-binding domain (RBD). After ACE-2 engagement, the S2' site is exposed and cleaved by transmembrane protease, serine 2 (TMPRSS2) at the cell surface or by cathepsin L within the endosome (8). After S2' cleavage, the fusion peptide is released, leading to fusion of viral and cellular membranes at the cell surface or within the endosome, respectively, followed by the release of viral RNA into the target cell (9). During SARS-CoV-2 evolution, the mode of entry has shifted from direct TMPRSS2-mediated fusion to cathepsin L-mediated endocytosis. While the initial Wuhan strain, European wild-type (D614G), Alpha, and Delta variants entered cells mainly by direct fusion, VOC Omicron appears to favor endocytosis (9–14). This change in phenotype was associated with a lower pathogenicity of the Omicron strains in murine and hamster models (12, 13, 15, 16).

The link between the route of entry and SARS-CoV-2 pathogenicity, however, has recently been questioned. In a murine knockout model, TMPRSS2 was shown to be critical for SARS-CoV-2 entry in respiratory epithelia, including Omicron (17). In a similar model, TMPRSS2 was required for the spread of VOCs Beta and Omicron in the upper and lower respiratory tract (18). These data are supported by results in human respiratory and intestinal organoids, where infections with Omicron strains BA.1 and XBB1.5 were also dependent on TMPRSS2 (19). In addition, peptide-based

pan-coronavirus fusion inhibitors potentially blocked the entry of XBB and XBB.1.5 strains into lung-derived Calu-3 cells (20).

One explanation for this discrepancy may be that the usage of TMPRSS2 is different for the various Omicron subvariants. For example, BA.5 was recently shown to have a higher replication capacity and infectivity in nasal organoids than BA.1, associated with prominent syncytium formation and more efficient usage of TMPRSS2 (21). On the other hand, the infectivity and transmissibility of SARS-CoV-2 may be only partially reflected by the interaction of the viral spike protein with the cellular receptors for entry. In addition, a role of non-structural proteins (NSP) 6 and 12 in SARS-CoV-2 virulence has recently been described (22, 23).

Our goal was to elucidate how SARS-CoV-2 entry mechanisms evolved during the pandemic. Using nine clinical isolates, including five Omicron strains collected at different time points, we investigated viral entry in four human cell lines in the presence of an inhibitor of TMPRSS2-mediated fusion and a cathepsin protease inhibitor blocking viral endocytic entry. We focused on variant-specific amino-acid substitutions that may alter entry pathways and contribute to SARS-CoV-2 pathogenesis.

2 Materials and methods

2.1 Cell culture

SARS-CoV-2 strains were propagated in human Calu-3, Caco-2 (CLS Cell Lines Service, Eppenheim, Germany), A549^{hACE2+/TMPRSS2+} (InvivoGen, San Diego, US), and HEK293T cell lines using DMEM (Gibco, Waltham, MA) supplemented with 1% streptomycin/penicillin and 10% fetal calf serum (Pan Biotech, Aidenbach, Germany). Calu-3 and Caco-2 cells support SARS-CoV-2 cell entry mainly via ACE-2/TMPRSS2-mediated direct fusion (9, 24, 25), while cathepsin L-mediated endocytosis is preferentially used in A549^{hACE2+/TMPRSS2+} and HEK293T cells (24, 26, 27). Cells were split twice weekly and tested quarterly for mycoplasma contamination. The day before infection, cells were plated at a concentration of 15,000 cells/well in 96-well-plates.

2.2 Viruses

European wild-type strain CJ (B.1.1, GenBank accession no. PP125281) was isolated during the first SARS-CoV-2 wave in Germany (April 2020). VOC Alpha (B.1.1.7 Q27*K68*, PP125282, January 2021; B.1.1.7 Q27*, PP125283, February 2021) and Delta isolates (originally designated B.1.617.2, OK149285, June 2021; now AY.33 according to the most recent classification) were obtained during the second and third SARS-CoV-2 wave (28), respectively. Five VOC Omicron strains (BA.1.17.2, PP125291, January 2022; BA.1.1, PP125284, February 2022; BA.2.9, PP125292, March 2022; BE.1.1, PP125294, June 2022; BA.5.1, PP125293, June 2022) were isolated subsequently. The collection of patients' respiratory samples was approved by the Ethical Commission at the Faculty for Medicine, University of Regensburg (COVUR study, Ref. no. 20-1785-101 from April 9, 2020).

Viruses were isolated on different cell lines (see above) using 1% amphotericin B (PAN Biotech, Aidenbach, DE) and 0.01% vancomycin (Hikma Pharmaceuticals, London, UK) to prevent fungal and bacterial infection. Viral replication was monitored using RT-qPCR (see below) for two to seven days post infection. Viral supernatants were harvested at the suspected peak of viral replication, purified through 0.22 μ m pore size filters (Carl Roth GmbH, Karlsruhe, DE), and frozen in aliquots at -80 °C. Cell culture experiments were performed under biosafety level 3 conditions according to regulatory requirements. The TCID₅₀ was determined using limiting dilution in 96-well-plates according to the method of Reed and Munch (1938).

2.3 Inhibitors

Aloxistatin and camostat (both MedChemExpress, Monmouth Junction, NJ) were used at concentrations of 0.024-100 μ M to inhibit SARS-CoV-2 endocytic uptake and direct TMPRSS2-mediated fusion on the cell surface, respectively. Inhibitors were used as single agents or in combination as a 1:1 mixture. The toxicity of both drugs at the indicated concentrations was determined using the 3-(4,5-dimethylthiazol-2-yl)-2,5-diphenyl-tetrazolium bromide (MTT) assay (Supplementary Figure S1), as described previously (29). Cells were preincubated with the inhibitors for 1 hour before infection, using an MOI of 0.015 for each virus isolate. To reduce the input virus, cell culture supernatants were replaced with fresh medium containing the respective inhibitor concentrations at 12-16 hours post infection (p.i.), without performing additional washing steps. This procedure resulted in an average reduction of the viral background by two to three orders of magnitude (Supplementary Figure S2). Final viral loads were determined two days p.i.. Viral strains with less than 0.5 log₁₀ RNA copies/ml above background control in the absence of inhibitors were classified as non-replicative in this cell line. The experiments were conducted in at least three completely independent runs, and results are presented as mean values with the standard error.

2.4 Determination of viral load

Cell culture supernatants were mixed with an equal amount of DLR buffer (0.1 M NaCl, 0.01 M Tris, 0.5% IGEPAL CA-630 in DEPC H₂O, pH 7.4) plus RNase inhibitor (Applied Biosystems, Darmstadt, Germany) (30). After 30 min, RT-qPCR was performed using a published protocol on a StepOnePlus Real-time PCR system (31). *In vitro* transcribed RNA served as reference for quantification (32). Controls included cells without inhibitor and without virus ("cell control"), cells without inhibitor and with virus ("virus control, VC"), and cells fixed with 4% PFA (Sigma-Aldrich, St. Louis, MO) ("background control, BC"). The latter were washed five times with DPBS and infected in parallel on separate plates to prevent evaporation and interference with non-fixed cell layers and viruses.

2.5 Next generation sequencing

NGS was performed with RNA extracted from respiratory specimen using the EZ1 Advanced XL platform (Qiagen, Hilden, Germany) (29). Viral load was quantified using the real-time PCR described above. After normalizing viral copy numbers, SARS-CoV-2 RNA was reverse-transcribed using the IonTorrent™ NGS Reverse Transcription Kit (Thermo Fisher Scientific, Waltham, USA) and amplified in 247 separate amplicons using the Ion AmpliSeq™ SARS-CoV-2 Insight Research Assay (Thermo Fisher Scientific, Waltham, USA). The sequencing libraries were automatically prepared by the IonChef™ instrument (Thermo Fisher Scientific) and quantified on a LightCycler 480 II instrument (Roche Diagnostics, Mannheim, Germany) using the Ion Library TaqMan™ Quantitation Kit. After high-throughput sequencing on the IonTorrent™ Genestudio S5 Plus instrument (Thermo Fisher Scientific), basecalling and demultiplexing were performed using the Torrent Suite 5.18. Processed reads were further analyzed using the SARS-CoV-2 Research Plug-in Package and aligned to the SARS-CoV-2 MN908947 (Wuhan-Hu-1) reference genome. Consensus sequences using the generateConsensus v5.16.0.10 were generated applying a minimum read depth of 20 and a maximum of 5 percent ambiguous bases. Single nucleotide polymorphisms, detected by variantCaller v5.18.0, were annotated with COVID19AnnotateSnpEff v5.16.0.5.

For isolates Omicron (BA.1.1), Omicron (BA.1.17.2), Omicron (BE.1.1), and Omicron (BA.5.1), gaps of 30-50 N-bases with a sequencing depth below the cutoff were filled by re-sequencing using the Midnight Expansion Kit, which generates overlapping 1,200 bp PCR products. The resulting amplicon libraries were sequenced on a MinION Mk1B instrument using the Rapid Barcoding Kit V14 and an R10.4.1 flow cell (Oxford Nanopore Technologies, Oxford, UK). Consensus sequences were generated using the epi2me-labs wf-artic nextflow command line workflow with default parameters.

SARS-CoV-2 isolates were assigned to the PANGO designation based on the SARS-CoV-2 mutation analysis (pangolin-data v1.23.1, release October 27, 2023) of the Stanford Coronavirus

Antiviral & Resistance Database (<https://covdb.stanford.edu/sierra/sars2/by-patterns/>, accessed on January 11, 2024) (33). Amino acids were numbered according to the GISAID CoV mutation App (<https://gisaid.org/>).

2.6 Phylogeny and statistics

The phylogenetic relationship of the nine virus strains was determined by analyzing the full-length nucleotide sequences using the open-source platform Nextclade v3.1.0 (<https://clades.nextstrain.org/>). The contribution of cathepsin-mediated endocytosis and TMPRSS2-mediated fusion to viral entry was expressed as percentage of the inhibition by the combined blockade with camostat and aloxistatin based on the viral load (VL) determined at the non-toxic inhibitor concentration of 25 μ M using the following equation: $\frac{\log_{10} VL_{VC} - \log_{10} VL_{inhibitor}}{\log_{10} VL_{VC} - \log_{10} VL_{mixture}}$, where inhibitor means aloxistatin or camostat, respectively, and “mixture” means a 1:1 ratio of both inhibitors. Statistics was performed using two-way ANOVA with Šidák’s correction to account for multiple comparisons.

3 Results

3.1 Isolation of different SARS-CoV-2 strains in the course of the pandemic

From April 2020 until June 2022, we isolated nine different SARS-CoV-2 strains out of 86 respiratory samples of patients being treated at the University Hospital Regensburg. Phylogenetic analysis using the platform Nextclade revealed that the nine strains of our study, which reflected the course of the pandemic, clustered with their respective clades (Figure 1).

3.2 Omicron strains are more susceptible to blockers of cathepsin-mediated endocytosis than Alpha and Delta strains

The route of entry of the nine viral strains was studied using four different cell lines. The inhibitors aloxistatin and camostat were non-toxic as single agents or in combination in all four cell lines up to a concentration of 25 μ M (Supplementary Figure S1). In the absence of inhibitors, all strains showed an efficient replication in Calu-3 and Caco-2 cells with viral loads ranging from 10^9 – 10^{10} RNA copies/ml within 48 hours p.i. (Figure 2). The combination of both inhibitors reduced viral replication of all strains to background level. The two Alpha strains, which were genetically identical except for one mutation in ORF3, behaved similarly. Aloxistatin was less effective than the mixture in blocking European wild-type, Alpha, Delta, and Omicron strains in most assays. In addition, aloxistatin inhibited BA.1.17.2, BA.2.9 and BE.1.1 entry in Calu-3 cells less effectively than camostat, indicating that the reduction in viral load by camostat, resulting from its inhibition of TMPRSS2-mediated fusion, was also more pronounced in the Omicron strains.

In A459^{hACE2+/TMPRSS2+} cells, SARS-CoV-2 strains replicated with viral loads ranging from 10^6 – 10^9 RNA copies/ml (Figure 2). The early (BA.1.17.2, BA.1.1) in contrast to the later Omicron strains (BA.2.9, BE.1.1, BA.5.1) were unable to replicate in this cell line. Alpha and Delta strains were blocked more strongly by camostat, whereas both inhibitors were similarly active against Omicron strains BA.2.9 and BE.1.1. BA.5.1 was preferentially blocked by aloxistatin. The mixture of both inhibitors resembled the inhibitory effect of camostat in Alpha and Delta strains, but was more effective than the individual inhibitors in Omicron strains.

In HEK293T cells, which predominantly support endocytic entry, only two variants (BE1.1, BA.5.1) showed substantial replication and were inhibited more effectively by aloxistatin than

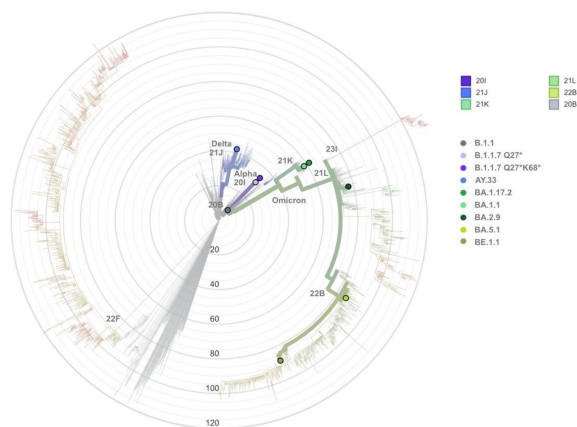


FIGURE 1

Phylogenetic analysis of the nine SARS-CoV-2 strains of our study using the open-source platform Nextclade (<https://clades.nextstrain.org/>). The individual strains (European wild-type B.1.1/20B (black), Alpha variants B.1.1.7 Q27*/20I (light purple) and B.1.1.7 Q27*K68*/20I (dark purple), Delta variant AY.33/21J (blue), as well as Omicron strains BA.1.17.2/21K, BA.1.1/21K, BA.2.9/21L, BE.1.1/22B, and BA.5.1/22B (green color panel), designated to PANGO lineages and Nextstrain clades, respectively, are incorporated into a radial phylogenetic reference tree and are identified by colored dots. Clades 22F and 23I include SARS-CoV-2 strains XBB and BA.2.86/JN.1., respectively. The radius of the circles reflects the number of mutations between the SARS-CoV-2 variants. The phylogenetic relationships between the strains are shown as bold branches.

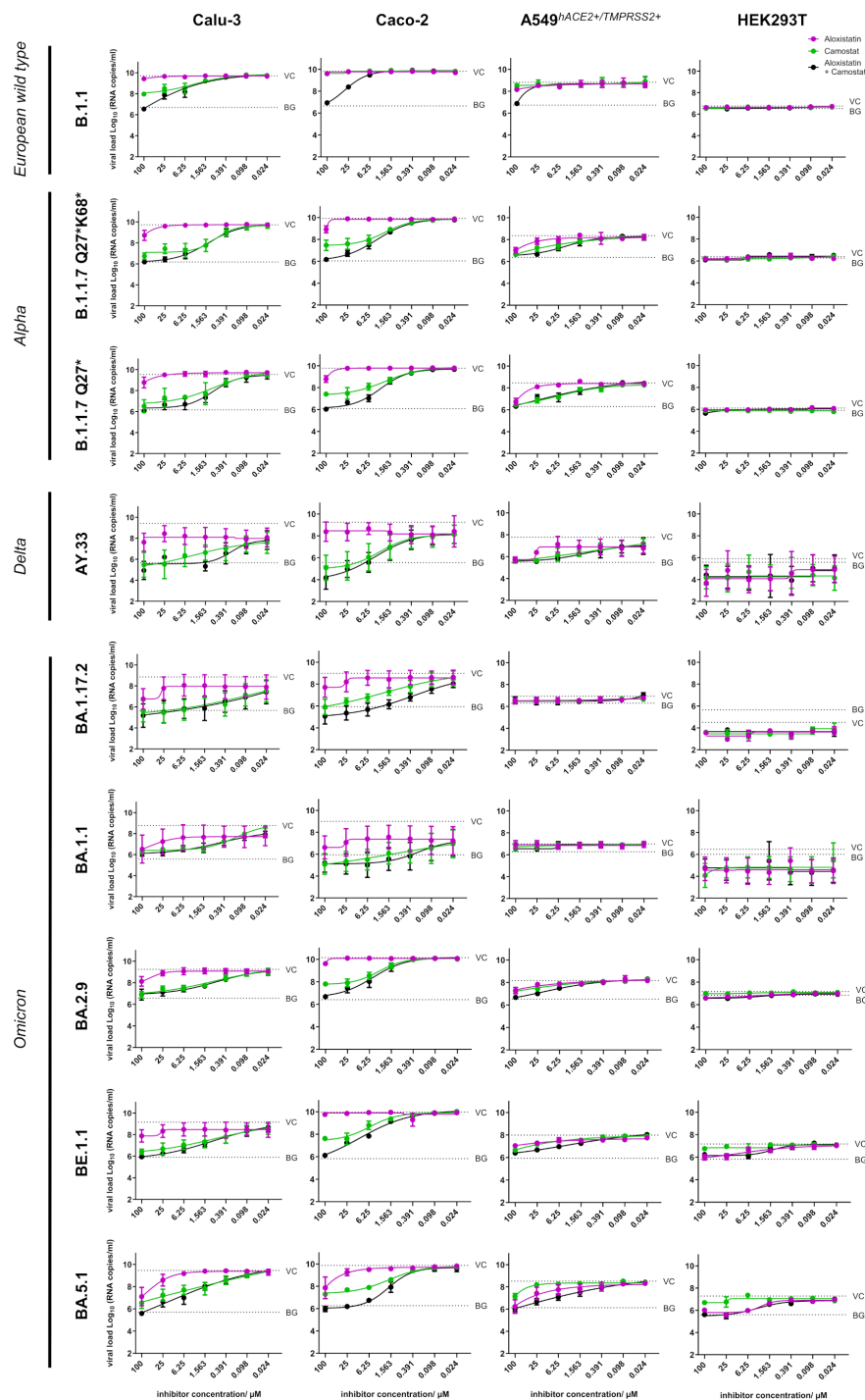


FIGURE 2

Susceptibility of the nine different SARS-CoV-2 strains to inhibitors of TMPRSS2-mediated fusion and cathepsin-mediated endocytosis. SARS-CoV-2 European wild-type (B.1.1), variant-of-concern (VOC) Alpha (B.1.1.7 Q27*K68*, B.1.1.7 Q27*), Delta (AY.33), and Omicron (BA.1.17.2, BA.1.1, BA.2.9, BE.1.1, BA.5.1) were propagated in four human cell lines (Calu-3, Caco-2, A549^{hACE2+/TMPRSS2+}, HEK293T) in the presence of increasing concentrations (0.024–100 μ M) of camostat, an inhibitor of TMPRSS2-mediated viral direct fusion with cellular membrane (green curve), aloxistatin, an inhibitor of cathepsin-mediated viral endocytic uptake (pink curve), and a 1:1 mixture of both inhibitors (black curve). Viral load was determined in cell culture supernatants 48h p.i. using RT-qPCR and are presented as \log_{10} RNA copies/ml. Controls included cells infected with SARS-CoV-2 in the absence of inhibitors (“virus control”, VC), and cells fixed with 4% paraformaldehyde and exposed to SARS-CoV-2 (“background control”, BG), shown as dashed horizontal lines. Data show mean and standard error of three independent experiments.

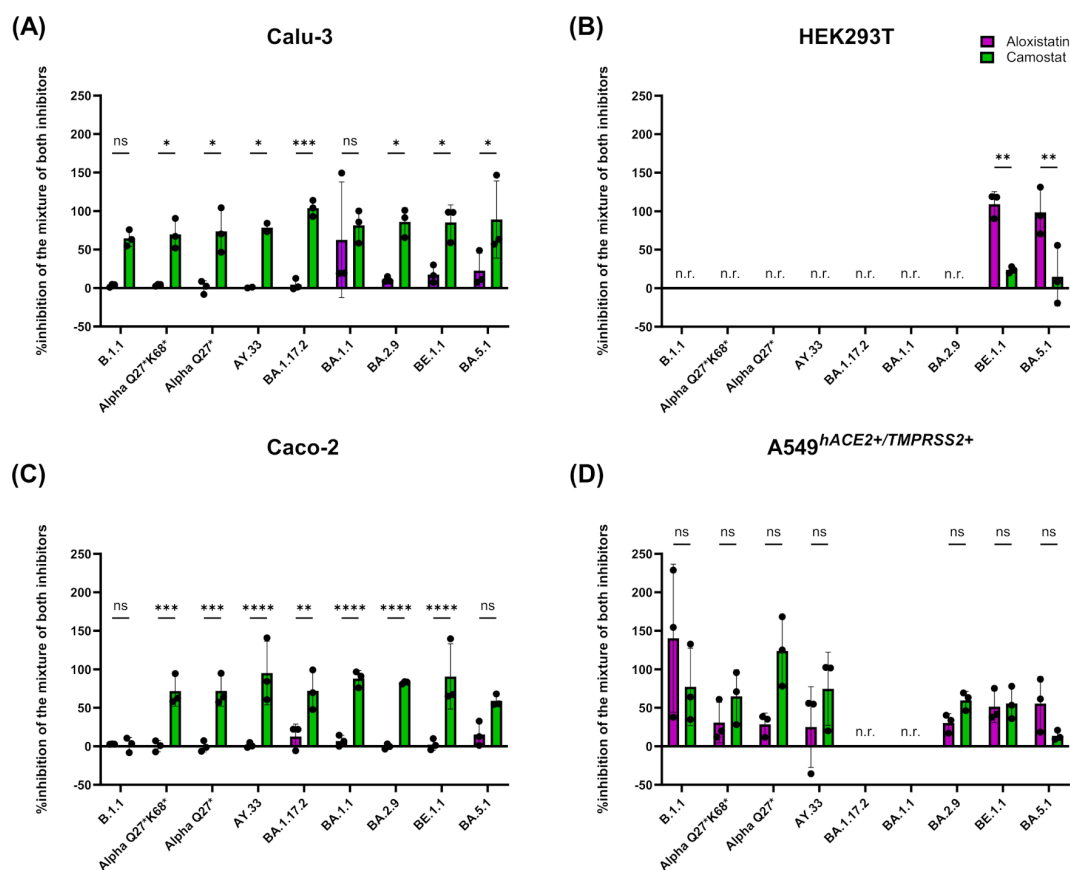


FIGURE 3

Degree of direct TMRPSS2-mediated fusion and cathepsin-mediated endocytic uptake of the nine different SARS-CoV-2 strains in four different cell lines. Calculation of the reduction in viral load induced by aloxistatin (pink columns) and camostat (green columns) at the non-toxic concentration of 25 μ M as % inhibition induced by the mixture of the two inhibitors for Calu-3 cells (A), HEK293T cells (B), Caco-2 cells (C) and A549^{hACE2+/TMPRSS2+} cells (D). A higher percentage indicates a stronger role of the respective mode of entry for the respective virus strain. In A549^{hACE2+/TMPRSS2+} cells, strains BA.1.17.2 and BA.1.1 were non-replicative (n.r.). In HEK293T cells, virus replication was observed for strains BE.1.1 and BA.5.1 only. Statistics was performed using two-way ANOVA with Sidák's correction to account for multiple comparisons. * $p < 0.05$, ** $p < 0.01$, *** $p < 0.001$, **** $p < 0.0001$.

by camostat (Figures 2, 3B). The mixture of both inhibitors was just as active as aloxistatin alone. When summarizing the results in all cell lines, the two most recent Omicron strains in our panel were more sensitive to inhibition of cathepsin-mediated endocytosis than the other strains, but still sensitive to inhibition of direct TMRPSS2-mediated fusion.

3.3 Increase and decrease in SARS-CoV-2 TMRPSS2-mediated entry during the course of the pandemic

In order to directly compare the degree of cathepsin-mediated endocytosis or TMRPSS2-mediated fusion of all virus strains, we calculated the reduction in viral load by aloxistatin or camostat at 25 μ M as the percentage of the inhibition by the combined inhibitor blockade (Figure 3). In Calu-3 and Caco-2 cells, all strains except for two were inhibited significantly better by camostat than by aloxistatin ($p < 0.05$, Figure 3A, and $p < 0.01$, Figure 3C), whereas the opposite was the case for the replicative strains BE.1.1 and BA.5.1 in HEK293T cells ($p < 0.01$) (Figure 3B). In A549^{hACE2+/TMPRSS2+} cells, camostat blocked

Alpha Q27* and Delta AY.33 more efficiently than aloxistatin, while two of the three replicating Omicron variants responded similarly to both inhibitors; BA.5.1, in particular, showed enhanced endocytic entry reflected by stronger inhibition by aloxistatin (Figure 3D).

Overall, the results showed a trend in which entry of clinical SARS-CoV-2 isolates via TMRPSS2-mediated membrane fusion into Calu-3 and Caco-2 cell lines remained relatively constant over the course of the pandemic. In contrast, entry via endocytosis appeared to increase with the emergence of VOC Omicron.

3.4 Endocytic uptake preferentially utilized by strains carrying $\Delta 69/\Delta 70$, L452R, and F486V

To correlate the mode of entry of the nine SARS-CoV-2 strains with the amino acid sequence in the viral spike protein, we analyzed the patients' virus isolates using NGS. The wild-type strain of our study carried D614G in the spike protein as described for European strains at the beginning of the SARS-CoV-2 pandemic (34).

Over the course of the pandemic, the number of amino acid substitutions increased in 17 SARS-CoV-2 NSPs (Figure 4B), while seven (NSP7, NSP8, NSP9, NSP10, NSP11, NSP16, and ORF6) remained unaffected. Amino acid exchanges that occurred in at least three viral strains were localized in NSP1 (S135R), NSP3 (T24I, G489S), NSP4 (L264F, T327I, T492I), NSP5 (P132H), NSP6 (Δ 106, Δ 107, Δ 108), NSP12 (P323L), NSP13 (R392C), NSP14 (I42V), NSP15 (T112I), ORF3 (T223I) and in structural proteins E (T9I), M (A62T, Q219E), and N (P13L, Δ 31-33, R203, G204R, S413R).

Most of these amino acid substitutions occur in the context of Omicron evolution. Amongst them, Δ 106–108 and I189V in NSP6 (22) and P323L/G671S or P323L in NSP12 (23) were associated with increased SARS-CoV-2 replication in the upper respiratory tract. In our data set, all strains harbored P323L in NSP12, and therefore the differences in entry observed among the Omicron strains cannot be attributed to this substitution. Deletions in NSP6 were observed in the two earlier (Δ 106-107) and in the three most recent Omicron strains (Δ 106-108), but did not discriminate between more TMPRSS2-dependent (BA.1.17.2, BA.1.1, BA.2.9) and more cathepsin-dependent strains (BA.5.1, BE.1.1). More notable was amino acid substitution D3N in the M protein, a prototypic mutation for BA.4/BA.5 strains (36), which was also observed in the endocytotic BE.1.1 and BA.5.1 strains of our study, while the more TMPRSS2-dependent isolates carried D or G at this position.

4 Discussion

Our study used nine clinical SARS-CoV-2 strains obtained over the course of the pandemic to investigate how viral entry mechanisms evolved over time. Other groups used pseudotyped virions (37), which are perfectly suited to compare the effect of different spike proteins and distinct amino acid substitutions on entry. Pseudotyped viruses, however, do not complete the viral life cycle and do not reflect the effect of genes outside the spike protein. Therefore, we have obtained SARS-CoV-2 wild-type, Alpha and Delta isolates, and five additional strains from the difficult-to-isolate VOC Omicron (10, 11, 16). These strains enabled us to analyze the susceptibility to fusion inhibitor camostat and endocytosis blocker aloxistatin using live virus assays, which better reflect virus biology than single-replication assays. However, there are limitations to this approach, as tests with replicative viruses cannot distinguish between the role of entry and replication, which may lead to confounding effects. In addition, efficient isolation in cell culture may result in the selection of particularly infectious viral strains that do not adequately reflect the majority of circulating viruses. Furthermore, primary virus isolates may not be equally replicative in different cell lines, as we observed for BA.1.1 carrying spike mutation R346K, which showed reduced fitness in Calu-3 cells. This phenomenon was also observed by others (13) and could explain the variable infectivity of this strain in Calu-3 cells.

In the two cell lines with high-level expression of fusion-associated TMPRSS2 (Calu-3, Caco-2) (9, 24, 25), wild-type, Alpha, Delta and

most Omicron strains were efficiently blocked by camostat but not by aloxistatin. These results confirm data by others showing that TMPRSS2 is not only used by early SARS-CoV-2 VOCs, but is also required for the entry of pseudotyped Omicron strains into Calu-3 cells *in vitro* (14, 19). In contrast, other studies report that the entry of Omicron into Calu-3 occurs predominantly through endocytosis and that direct TMPRSS2-mediated fusion plays a particularly important role *in vivo* (17). The inhibitory effect of aloxistatin was more pronounced in the cell lines supporting endosomal uptake of SARS-CoV-2 (A549^{hACE2+/TMPRSS2+}, HEK293T) (24, 26). While Alpha and Delta strains were predominantly dependent on direct fusion in A549^{hACE2+/TMPRSS2+} cells, we observed an increasing sensitivity to aloxistatin in the two most recent Omicron BE.1.1 and BA.5.1 strains, consistent with recent findings by Willett et al. (14). For these strains, we noticed an effective utilization of the cathepsin-dependent entry pathway in HEK293T cells. In conclusion, all SARS-CoV-2 strains analyzed in our study retained the ability for direct fusion, and Omicron isolates were additionally capable to enter via endocytosis. Thus, SARS-CoV-2 appears to have expanded rather than shifted its cell tropism over the course of the pandemic.

Notably, our five Omicron sublineages differed in viral entry, which is explained by the large genetic variability between these isolates. Accordingly, sequence analyses have shown that these viruses are grouped in different branches of the phylogenetic tree (Figure 1). This evolution has been linked to immunological pressure from large-scale infection and/or vaccination that drove the diversification of SARS-CoV-2 spike proteins (38). By generating spike chimeras, Strobelt and colleagues showed that Omicron's F375 reduced infectivity, and Omicron's Y655, K764, K856, and K969 amino acid exchanges decreased TMPRSS2 dependency and supported endosomal entry (37). Similar data were reported by Qu et al., who demonstrated K547 and Y655 amino acid substitutions to be responsible for the low fusogenicity and enhanced endosomal uptake of Omicron (39). Khatri et al. associated the amino acid substitution H681 in Omicron (as opposed to R681 in Delta) with a lower fusion rate (40). The Omicron strains in our study carried all (BA.1.17.2, BA.1.1) or five of these substitutions (BA.2.9, BE.1.1, BA.5.1), but this did not explain the differences in TMPRSS2-mediated fusion and cathepsin-mediated endocytosis within our Omicron strains.

When correlating the mode of entry with the amino acid sequence of the viral spike protein, F486V (in the context of Δ 69/ Δ 70 and L452R) was the only amino acid exchange in the two virus isolates (BE.1.1, BA.5.1) that were able to replicate in HEK293T cells and showed stronger inhibition by aloxistatin than the other VOCs. F486V was described as an escape mutation in response to neutralizing antibodies triggered by immune responses to Omicron subvariants or Omicron-based vaccine booster (41, 42). In conjunction with the Delta marker mutation L452R, F486V appears to contribute to the enhanced replicative fitness and syncytium formation of Omicron BA.5 in nasal airway organoids (21). In the pseudotype model, the combination of Δ 69/ Δ 70, L452R, and F486V introduced by targeted mutagenesis contributed to reduced infectivity in Caco-2 cells, but enhanced infectivity in

A549^{hACE2+} and in A549^{hACE2+/TMPRSS2+} cells (43). This phenotype may, at least in part, be explained by an increased propensity of this strain to use the endocytic entry pathway, while TMPRSS2-dependent entry remains preserved.

Recently, the WHO classified JN.1 ('Juno') as a variant of interest (VOI) and XFG as a variant under monitoring (VUM). Both lineages are now widespread across multiple countries and show extensive diversification into sublineages, while harboring a remarkably high number of Spike mutations (44). Among these are the combinations $\Delta 69/\Delta 70$ and L452R with F486S in XBB.1, F486P in XBB.1.6 and JN.1, and F486P/N487D in XFG. Notably, the epidemiological history demonstrates that this specific mutation pattern, identified in BE.1.1 and BA.5.1 in 2022, has since become dominant in currently circulating variants, supporting the notion that expansion of the endocytic entry pathway confers a selective advantage in terms of enhanced transmissibility.

To date, available data do not indicate that these variants are associated with increased morbidity or mortality in infected individuals. This is most likely due to the widespread development of robust immunity within the population as a result of vaccination or prior infection. Nevertheless, careful monitoring—particularly in immunocompromised patients—remains warranted, since these variants still retain the capacity for TMPRSS2-dependent infection and may therefore cause severe disease of the lower respiratory tract.

The pathogenicity of SARS-CoV-2 cannot be attributed solely to its entry mechanisms or to amino acid substitutions in the spike protein. Remarkably, not all viral genes in our study accumulated mutations during viral evolution. Genes that remained conserved include cofactors of essential RNA replication machinery (NSP7, NSP8, NSP10) and RNA-binding or cap-forming proteins (NSP9, NSP16) (3, 45). In contrast, amino acid substitutions in the viral isolates of our study predominantly affected genes involved in viral replication (NSP4, NSP6, NSP12, NSP13, NSP14), interferon antagonism (NSP3, NSP5, NSP15, ORF3b), host shut-off (NSP1) and autophagy (ORF3a), as well as structural proteins (S, E, M, and N). Consequently, SARS-CoV-2 adaptation to the human host appears to focus on evasion of innate and adaptive immunity, refinement of entry pathways, and optimization of replication efficiency, while core components of the RNA replication machinery remain conserved.

The study by Chen et al. highlighted that amino acid substitutions in NSP6 contribute to a more benign phenotype (22) by promoting more efficient formation of double-membrane vesicles (46) and by reducing pyroptosis (47). In particular, Δ SGF in NSP6 represents an adaptation to replication in humans (48), and, as a gain-of-function change, strengthens the interaction between NSP3 and NSP4 during double-membrane vesicle formation (46). Δ SGF was present in most of our viral isolates and thus does not account for the observed differences between TMPRSS2-dependent and endocytic strains. However, another mutation, M:D3N – prototypical for BA.4/BA.5 lineages (36) – was detected exclusively in the two most endocytic Omicron strains replicating in HEK293T cells (BE.1.1 and BA.5.1). Thus, M:D3N may represent an additional candidate – alongside the spike mutations $\Delta 69/\Delta 70$, L452R, and F486V – that facilitates endocytic entry and warrants further investigation.

Altogether, our study investigated nine SARS-CoV-2 strains isolated throughout the pandemic in four different cell lines. Our data show that viral evolution has broadened the viral entry by shifting the balance toward increased endocytic uptake while preserving TMPRSS2-mediated fusion.

Limitations of the research

One limitation of our study is that experiments using replication-competent viruses do not allow a clear distinction between effects on viral entry and subsequent intracellular replication. Consequently, the observed effects – particularly in HEK293T cells – may reflect a combination of both processes rather than viral entry alone. A further limitation is that two of the cell lines used (Caco-2, HEK293T) are not of respiratory origin. As such, they may not fully capture the physiological complexity of the *in vivo* situation. In addition, all cell lines employed in this study are immortalized rather than primary cells, which may further limit the direct translational relevance of the findings.

Data availability statement

The datasets presented in this study can be found in online repositories. The names of the repository/repositories and accession number(s) can be found in the article/[Supplementary Material](#).

Ethics statement

The studies involving humans were approved by Ethical Commission at the Faculty for Medicine, University of Regensburg. The studies were conducted in accordance with the local legislation and institutional requirements. The participants provided their written informed consent to participate in this study.

Author contributions

CM: Data curation, Methodology, Visualization, Conceptualization, Writing – review & editing, Supervision, Formal Analysis. ZH: Writing – review & editing, Methodology. AH: Formal Analysis, Methodology, Data curation, Writing – review & editing. LA: Methodology, Writing – review & editing. HM: Writing – review & editing, Methodology. AL: Writing – review & editing, Methodology. FH: Investigation, Writing – review & editing. TD: Investigation, Writing – review & editing. RS: Investigation, Writing – review & editing. ML: Writing – review & editing, Investigation. TM: Writing – review & editing, Investigation. DL: Writing – review & editing, Investigation. FH: Investigation, Writing – review & editing. SS: Investigation, Writing – review & editing. MM: Writing – review & editing, Resources. HP: Resources, Writing – review & editing. BG: Writing – review & editing, Resources. BeS: Resources, Writing – review & editing.

AG: Writing – review & editing, Resources. BaS: Writing – review & editing, Supervision, Writing – original draft, Conceptualization, Funding acquisition. PS: Data curation, Conceptualization, Writing – review & editing, Methodology, Funding acquisition, Formal Analysis.

Funding

The author(s) declared that financial support was received for this work and/or its publication. This research was funded by the Bavarian Ministry of Science and Art as part of the pandemic responsiveness fund.

Acknowledgments

We thank Sakhila Ghimire and Simone Reichelt-Wurm for contributing Caco-2 and Calu-3 cells, respectively.

Conflict of interest

The authors declared that this work was conducted in the absence of any commercial or financial relationships that could be construed as a potential conflict of interest.

References

- Zhou P, Yang XL, Wang XG, Hu B, Zhang L, Zhang W, et al. A pneumonia outbreak associated with a new coronavirus of probable bat origin. *Nature*. (2020) 579:270–3. doi: 10.1038/s41586-020-2012-7
- Wu F, Zhao S, Yu B, Chen YM, Wang W, Song ZG, et al. A new coronavirus associated with human respiratory disease in China. *Nature*. (2020) 579:265–9. doi: 10.1038/s41586-020-2008-3
- Corman VM, Landt O, Kaiser M, Molenkamp R, Meijer A, Chu DK, et al. Detection of 2019 novel coronavirus (2019-nCoV) by real-time RT-PCR. *Euro Surveill*. (2023) 25(3):2000045. doi: 10.2807/1560-7917.ES.2020.25.3.2000045
- Jassat W, Abdool Karim SS, Mudara C, Welch R, Ozougwu L, Groome MJ, et al. Clinical severity of COVID-19 in patients admitted to hospital during the omicron wave in South Africa: a retrospective observational study. *Lancet Glob Health*. (2022) 10:e961–e9. doi: 10.1016/S2214-109X(22)00114-0
- Davies NG, Jarvis CI, Group CC-W, Edmunds WJ, Jewell NP, Diaz-Ordaz K, et al. Increased mortality in community-tested cases of SARS-CoV-2 lineage B.1.1.7. *Nature*. (2021) 593:270–4. doi: 10.1038/s41586-021-03426-1
- Wu Y, Pan Y, Su K, Zhang Y, Jia Z, Yi J, et al. Elder and booster vaccination associates with decreased risk of serious clinical outcomes in comparison of Omicron and Delta variant: A meta-analysis of SARS-CoV-2 infection. *Front Microbiol*. (2023) 14:1051104. doi: 10.3389/fmicb.2023.1051104
- Nevejan L, Ombelet S, Laenen L, Keyaerts E, Demuyser T, Seyler L, et al. Severity of COVID-19 among hospitalized patients: omicron remains a severe threat for immunocompromised hosts. *Viruses*. (2022) 14:2736. doi: 10.3390/v14122736
- Jackson CB, Farzan M, Chen B, Choe H. Mechanisms of SARS-CoV-2 entry into cells. *Nat Rev Mol Cell Biol*. (2022) 23:3–20. doi: 10.1038/s41580-021-00418-x
- Hoffmann M, Kleine-Weber H, Schroeder S, Kruger N, Herrler T, Erichsen S, et al. SARS-CoV-2 cell entry depends on ACE2 and TMPRSS2 and is blocked by a clinically proven protease inhibitor. *Cell*. (2020) 181:271–80 e8. doi: 10.1016/j.cell.2020.02.052
- Meng B, Abdullahi A, Ferreira I, Goonawardane N, Saito A, Kimura I, et al. Altered TMPRSS2 usage by SARS-CoV-2 Omicron impacts infectivity and fusogenicity. *Nature*. (2022) 603:706–14. doi: 10.1038/s41586-022-04474-x
- Zhao H, Lu L, Peng Z, Chen LL, Meng X, Zhang C, et al. SARS-CoV-2 Omicron variant shows less efficient replication and fusion activity when compared with Delta variant in TMPRSS2-expressed cells. *Emerg Microbes Infect*. (2022) 11:277–83. doi: 10.1080/22221751.2021.2023329
- Halfmann PJ, Iida S, Iwatsuki-Horimoto K, Maemura T, Kiso M, Scheaffer SM, et al. SARS-CoV-2 Omicron virus causes attenuated disease in mice and hamsters. *Nature*. (2022) 603:687–92. doi: 10.1038/s41586-022-04441-6
- Shuai H, Chan JF, Hu B, Chai Y, Yuen TT, Yin F, et al. Attenuated replication and pathogenicity of SARS-CoV-2 B.1.1.529 Omicron. *Nature*. (2022) 603:693–9. doi: 10.1038/s41586-022-04442-5
- Willett BJ, Grove J, MacLean OA, Wilkie C, De Lorenzo G, Furnon W, et al. SARS-CoV-2 Omicron is an immune escape variant with an altered cell entry pathway. *Nat Microbiol*. (2022) 7:1161–79. doi: 10.1038/s41564-022-01143-7
- Yuan S, Ye ZW, Liang R, Tang K, Zhang AJ, Lu G, et al. Pathogenicity, transmissibility, and fitness of SARS-CoV-2 Omicron in Syrian hamsters. *Science*. (2022) 377:428–33. doi: 10.1126/science.abn8939
- Suzuki R, Yamasoba D, Kimura I, Wang L, Kishimoto M, Ito J, et al. Attenuated fusogenicity and pathogenicity of SARS-CoV-2 Omicron variant. *Nature*. (2022) 603:700–5. doi: 10.1038/s41586-022-04462-1
- Iwata-Yoshikawa N, Kakizaki M, Shiwa-Sudo N, Okura T, Tahara M, Fukushi S, et al. Essential role of TMPRSS2 in SARS-CoV-2 infection in murine airways. *Nat Commun*. (2022) 13:6100. doi: 10.1038/s41467-022-33911-8
- Metzdorf K, Jacobsen H, Greweling-Pils MC, Hoffmann M, Luddecke T, Miller F, et al. TMPRSS2 is essential for SARS-CoV-2 beta and omicron infection. *Viruses*. (2023) 15:271. doi: 10.3390/v15020271
- Mykytyn AZ, Breugem TI, Geurts MH, Beumer J, Schipper D, van Acker R, et al. SARS-CoV-2 Omicron entry is type II transmembrane serine protease-mediated in human airway and intestinal organoid models. *J Virol*. (2023) 97(8):e0085123. doi: 10.1128/jvi.00851-23
- Xia S, Jiao F, Wang L, Yu X, Lu T, Fu Y, et al. SARS-CoV-2 Omicron XBB subvariants exhibit enhanced fusogenicity and substantial immune evasion in elderly

Generative AI statement

The author(s) declared that generative AI was not used in the creation of this manuscript.

Any alternative text (alt text) provided alongside figures in this article has been generated by Frontiers with the support of artificial intelligence and reasonable efforts have been made to ensure accuracy, including review by the authors wherever possible. If you identify any issues, please contact us.

Publisher's note

All claims expressed in this article are solely those of the authors and do not necessarily represent those of their affiliated organizations, or those of the publisher, the editors and the reviewers. Any product that may be evaluated in this article, or claim that may be made by its manufacturer, is not guaranteed or endorsed by the publisher.

Supplementary material

The Supplementary Material for this article can be found online at: <https://www.frontiersin.org/articles/10.3389/fimmu.2025.1736891/full#supplementary-material>

- population, but high sensitivity to pan-coronavirus fusion inhibitors. *J Med Virol.* (2023) 95:e28641. doi: 10.1002/jmv.28641
21. Li C, Huang J, Yu Y, Wan Z, Chiu MC, Liu X, et al. Human airway and nasal organoids reveal escalating replicative fitness of SARS-CoV-2 emerging variants. *Proc Natl Acad Sci U S A.* (2023) 120:e2300376120. doi: 10.1073/pnas.2300376120
22. Chen DY, Chin CV, Kenney D, Tavares AH, Khan N, Conway HL, et al. Spike and nsp6 are key determinants of SARS-CoV-2 Omicron BA. 1 attenuation. *Nat.* (2023) 615:143–50. doi: 10.1038/s41586-023-05697-2
23. Kim SM, Kim EH, Casel MAB, Kim YI, Sun R, Kwak MJ, et al. SARS-CoV-2 variants with NSP12 P323L/G671S mutations display enhanced virus replication in ferret upper airways and higher transmissibility. *Cell Rep.* (2023) 42:113077. doi: 10.1016/j.celrep.2023.113077
24. Koch J, Uckelely ZM, Doldan P, Stanifer M, Boulant S, Lozach PY. TMPRSS2 expression dictates the entry route used by SARS-CoV-2 to infect host cells. *EMBO J.* (2021) 40:e107821. doi: 10.15252/embj.2021107821
25. Murgolo N, Therien AG, Howell B, Klein D, Koeplinger K, Lieberman LA, et al. SARS-CoV-2 tropism, entry, replication, and propagation: Considerations for drug discovery and development. *PLoS Pathog.* (2021) 17:e1009225. doi: 10.1371/journal.ppat.1009225
26. Ou X, Liu Y, Lei X, Li P, Mi D, Ren L, et al. Characterization of spike glycoprotein of SARS-CoV-2 on virus entry and its immune cross-reactivity with SARS-CoV. *Nat Commun.* (2020) 11:1620. doi: 10.1038/s41467-020-15562-9
27. Saccon E, Chen X, Mikaeloff F, Rodriguez JE, Szekely L, Vinhas BS, et al. Cell-type-resolved quantitative proteomics map of interferon response against SARS-CoV-2. *iScience.* (2021) 24:102420. doi: 10.1016/j.isci.2021.102420
28. Bauswein M, Peterhoff D, Plentz A, Hiergeist A, Wagner R, Gessner A, et al. Increased neutralization of SARS-CoV-2 Delta variant after heterologous ChAdOx1 nCoV-19/BNT162b2 versus homologous BNT162b2 vaccination. *iScience.* (2022) 25:103694. doi: 10.1016/j.isci.2021.103694
29. Magnus CL, Hiergeist A, Schuster P, Rohrhofer A, Medenbach J, Gessner A, et al. Targeted escape of SARS-CoV-2 *in vitro* from monoclonal antibody S309, the precursor of sotrovimab. *Front Immunol.* (2022) 13:966236. doi: 10.3389/fimmu.2022.966236
30. Shatzkes K, Teferedegne B, Murata H. A simple, inexpensive method for preparing cell lysates suitable for downstream reverse transcription quantitative PCR. *Sci Rep.* (2014) 4:4659. doi: 10.1038/srep04659
31. Corman VM, Landt O, Kaiser M, Molenkamp R, Meijer A, Chu DK, et al. Detection of 2019 novel coronavirus (2019-nCoV) by real-time RT-PCR. *Euro Surveill.* (2020) 25:2000045.
32. Hitzentbichler F, Bauernfeind S, Salzberger B, Schmidt B, Wenzel JJ. Comparison of throat washings, nasopharyngeal swabs and oropharyngeal swabs for detection of SARS-CoV-2. *Viruses.* (2021) 13:653. doi: 10.3390/v13040653
33. Tzou PL, Tao K, Pond SLK, Shafer RW. Coronavirus Resistance Database (CoV-RDB): SARS-CoV-2 susceptibility to monoclonal antibodies, convalescent plasma, and plasma from vaccinated persons. *PLoS One.* (2022) 17:e0261045. doi: 10.1371/journal.pone.0261045
34. Volz E, Hill V, McCrone JT, Price A, Jorgensen D, O'Toole A, et al. Evaluating the effects of SARS-CoV-2 spike mutation D614G on transmissibility and pathogenicity. *Cell.* (2021) 184:64–75.e11. doi: 10.1016/j.cell.2020.11.020
35. Parsons RJ, Acharya P. Evolution of the SARS-CoV-2 omicron spike. *Cell Rep.* (2023) 42:113444. doi: 10.1016/j.celrep.2023.113444
36. Zelyas N, Pabbaraju K, Croxen MA, Lynch T, McCullough E, Murphy SA, et al. Tracking SARS-CoV-2 Omicron lineages using real-time reverse transcriptase PCR assays and prospective comparison with genome sequencing. *Sci Rep.* (2023) 13:17478. doi: 10.1038/s41598-023-44796-y
37. Strobel R, Broennimann K, Adler J, Shaul Y. SARS-CoV-2 omicron specific mutations affecting infectivity, fusogenicity, and partial TMPRSS2-independency. *Viruses.* (2023) 15:1129. doi: 10.3390/v15051129
38. Focosi D, Quiroga R, McConnell S, Johnson MC, Casadevall A. Convergent evolution in SARS-CoV-2 spike creates a variant soup from which new COVID-19 waves emerge. *Int J Mol Sci.* (2023) 24:2264. doi: 10.3390/ijms24032264
39. Qu P, Evans JP, Kurhade C, Zeng C, Zheng YM, Xu K, et al. Determinants and mechanisms of the low fusogenicity and high dependence on endosomal entry of omicron subvariants. *mBio.* (2023) 14:e0317622. doi: 10.1128/mbio.03176-22
40. Khatri R, Siddiqui G, Sadhu S, Maithil V, Vishwakarma P, Lohiya B, et al. Intrinsic D614G and P681R/H mutations in SARS-CoV-2 VoCs Alpha, Delta, Omicron and viruses with D614G plus key signature mutations in spike protein alters fusogenicity and infectivity. *Med Microbiol Immunol.* (2023) 212:103–22. doi: 10.1007/s00430-022-00760-7
41. Moriyama S, Anraku Y, Taminishi S, Adachi Y, Kuroda D, Kita S, et al. Structural delineation and computational design of SARS-CoV-2-neutralizing antibodies against Omicron subvariants. *Nat Commun.* (2023) 14:4198. doi: 10.1038/s41467-023-39890-8
42. Li T, Luo D, Ning N, Wang X, Zhang L, Yang X, et al. An omicron-based vaccine booster elicits potent neutralizing antibodies against emerging SARS-CoV-2 variants in adults. *Emerg Microbes Infect.* (2023) 12:2207670. doi: 10.1080/22221751.2023.2207670
43. Pastorio C, Noetger S, Nchioua R, Zech F, Sparrer KMJ, Kirchhoff F. Impact of mutations defining SARS-CoV-2 Omicron subvariants BA.2.12.1 and BA.4/5 on Spike function and neutralization. *iScience.* (2023) 26:108299. doi: 10.1016/j.isci.2023.108299
44. Guo C, Yu Y, Liu J, Jian F, Yang S, Song W, et al. Antigenic and virological characteristics of SARS-CoV-2 variants BA.3.2, XFG, and NB.1.8.1. *Lancet Infect Dis.* (2025) 25:e374–e7. doi: 10.1016/S1473-3099(25)00308-1
45. V'kovski P, Kratzel A, Steiner S, Stalder H, Thiel V. Coronavirus biology and replication: implications for SARS-CoV-2. *Nat Rev Microbiol.* (2021) 19:155–70. doi: 10.1038/s41579-020-00468-6
46. Ricciardi S, Guarino AM, Giaquinto L, Polishchuk EV, Santoro M, Di Tullio G, et al. The role of NSP6 in the biogenesis of the SARS-CoV-2 replication organelle. *Nature.* (2022) 606:761–8. doi: 10.1038/s41586-022-04835-6
47. Sun X, Liu Y, Huang Z, Xu W, Hu W, Yi L, et al. SARS-CoV-2 non-structural protein 6 triggers NLRP3-dependent pyroptosis by targeting ATP6AP1. *Cell Death Differ.* (2022) 29:1240–54. doi: 10.1038/s41418-021-00916-7
48. Feng S, O'Brien A, Chen DY, Saeed M, Baker SC. SARS-CoV-2 nonstructural protein 6 from Alpha to Omicron: evolution of a transmembrane protein. *mBio.* (2023) 14:e0068823. doi: 10.1128/mbio.00688-23
49. Duan L, Zheng Q, Zhang H, Niu Y, Lou Y, Wang H. The SARS-CoV-2 spike glycoprotein biosynthesis, structure, function, and antigenicity: implications for the design of spike-based vaccine immunogens. *Front Immunol.* (2020) 11:576622. doi: 10.3389/fimmu.2020.576622